

## POROSITY PREDICTION OF I-FIELD IN THE NIGER DELTA AREA USING WELL-LOG DATA AND SEISMIC ATTRIBUTES

<sup>1</sup> V. Makinde, <sup>2\*</sup> R. Bello, <sup>3</sup> M. O. Omeike and <sup>1</sup> D. O. Aikhuele

<sup>1</sup>Department of Physics, Federal University of Agriculture, Abeokuta, Nigeria.

<sup>2</sup>Department of Physics, University of Port Harcourt, Port Harcourt, Nigeria

<sup>3</sup>Department of Mathematics, Federal University of Agriculture, Abeokuta, Nigeria.

\*Corresponding Author: e-mail: rasaq.bello@uniport.edu.ng, Phone: +2348036684498.

Received: 09-02-16

Accepted: 14-04-16

### ABSTRACT

*There are many important characteristics of formations within the subsurface that can be used to determine locations of hydrocarbon reservoirs below the earth surface. This work used the Porosity characteristics of formation to determine the locations of hydrocarbon reservoirs of I – field. The study was aimed at interpolating data from few wells using well-log data, geo-statistical analysis and seismic attributes to determine porosity values in order to overcome the problem of multiple well drilling. The study area, I-field, is located between latitudes 4.7950°N and 4.8186°N, longitudes 6.9595°E and 6.9800°E. Variogram analysis and Sequential Gaussian Simulation were used as the geo-statistical techniques for interpolation. From these techniques, multiple models were generated and the best porosity model which revealed the direction of increased porosity within I-field, as well as areas with high and low porosity variation across the field was selected. Seismic attributes were then incorporated with this model to increase the level of certainty and reliability of the prediction. A cross-plot analysis of the gamma ray log and porosity log showed high responses along the depth 2800 m closing contour on a fault plane with average porosity variation of 18 - 28% at the depth 3200m located at the centre of the field. The cross-plot analysis revealed an increase in porosity at areas where sandstones are located (gamma-ray values from 0-55). Porosity prediction showed that locations at depth 2800 m within the I-field are of high porosity of 28% and are therefore viable locations for sitting of wells and prospecting for hydrocarbons; while locations at depth 3200m are of comparatively low porosity of 18%.*

**Key words:** Porosity, Seismic Attributes, Lithology, Well Log, Hydrocarbon

### INTRODUCTION

The Niger-delta basin is not a single large field but is made up of many different single reservoir most of which are sandstone pockets trapped within hydrocarbon shale strata. Hydrocarbon fields in the Niger-delta are not large but are many, with 574 fields discovered (481 oil and 93 natural gas

fields) in this region (Wikipedia.com). The delta formed at the site of a rift triple junction is related to the opening of the southern Atlantic starting in the Late Jurassic and continuing into the Cretaceous (Tuttle *et al.*, 1999).

From conventional 3-D structural interpretation, it is possible to identify

structural traps (structural highs) particularly in the prolific hydrocarbon province of the Niger Delta where mobile shale tectonics of the over pressured Akata formation results in dip structures, growth faults and associated rollovers, faulted anticlines, among others (Doust and Omatsola, 1989). From depth maps of reservoir tops, areas of possible hydrocarbon accumulation or prospects where wells have not been drilled can also be identified. With the aid of related seismic attributes, it is possible to rank these prospects on the basis of lateral and vertical variation of lithofacies, porosity, and permeability across the reservoir (Ogiesoba, 2010).

The prediction of physical properties such as porosity from empirical correlations of multivariate linear regression between seismic attributes and well log data was introduced by numerous authors (Schultz *et al.*, 1994. Norkhamboot and Wongpornchai, 2012). A seismic attribute analysis can also be used to estimate physical properties such as porosity, permeability and others in a reservoir (Leiphart and Hart, 2001; Tebo and Hart, 2003).

In characterizing hydrocarbon reservoirs, estimating reserves, and developing models for the best extraction of hydrocarbons, it is useful to know the lithology (for example, relative amounts of shale and sand) and associated porosity of the rocks in the target interval. In regions where a large number of wells have been drilled, pattern-based recognition methods and simple empirical relationships can be used successfully to infer rock properties from seismic data. However, in regions of limited well control, it is difficult to make accurate lithology or porosity prediction using empirical

relationships derived from just a few wells (Alao *et al.*, 2014).

Hydrocarbons have been located in all the depobelts of the Niger Delta, in good quality sandstone reservoirs belonging to the main deltaic sequences. Most of the accumulations occur in the roll-over anticlines in the hanging wall of growth faults, where they may be trapped in either dip or fault closures (Doust and Omatsola, 1990). The hydrocarbons are found in multiple pay sands with relatively short columns and adjacent fault blocks which usually have independent accumulations (Doust and Omatsola, 1990).

Rouhani *et al.*, (1996) concluded that geostatistics offer a variety of spatial estimation procedures which are known as kriging. These techniques are commonly used for interpolation of points at unsampled locations and estimation of average block values. Kriging techniques provide a measure of accuracy in the form of an estimation variance. Kriging and co-kriging are geo-statistical interpolation methods {Deutsch (2002), Dubruble (1998), Kelkar and Perez (2002)}.

The general kriging formula is:

$$z_k = \sum_{i=1}^n \lambda_i \cdot z_i \quad (1)$$

where;

$z_k$  = estimated value from 'n' surrounding values

$\lambda_i$  = weighting coefficient on location 'i'

$z_i$  = Actual value on location 'i' (Malvic and Prskalo, 2008).

Norkhamboot and Wongpornchai, (2012) in their study that used seismic attribute analysis to predict porosity of reservoir

using seismic and well log data; an interesting sand layer was identified by the well log data. The acoustic impedance volume was created as an external attribute for seismic attribute analysis. It was noted that to improve the ability of porosity prediction, the best attributes of multi-attribute analysis should be computed using multilayer feed-forward neural network technique.

Bisht *et al.*, (2013) observed that the identification of reservoir distribution of fluvial channels depositional environments is a challenging task for field development planning. To accomplish this task an integrated approach is required, where seismic attributes along with the lithology logs and geological concept can be used to define facies away from the wells.

Alao *et al* (2014) combined both physical attributes and geometric attributes to predict the spatial distribution of porosity as a result of the relationship between the seismic reflection data and physical properties.

The aim of this work is to use the data obtained from seismic survey and well logs incorporated with seismic attributes for development studies, and also to detect high hydrocarbon pay-zones (sweet spots) in the field of study.

## **MATERIALS AND METHODS**

### **Study Area**

Material used for this research was a secondary data obtained from Chevron Nigeria Limited through the Department of Petroleum Resources, Nigeria, of the area of study. The data was acquired in I-field in the Nigeria Niger Delta. The following are the sets of data given by Chevron Nigeria Limited; Seismic survey data of the area to be studied, well log data of the six (6) wells

drilled within the area of study, check shot data, directional survey data, biostrat chart, and the well header data.

The software used in this research is the PETREL software (version 2011.2) developed by Schlumberger. An advanced quantitative methodology integrating 3D seismic data was adopted.

It has been said that porosity values can be determined from only well logs, although none of these logs actually measures pore volume directly, they can detect the contrast between the physical characteristics of water and rock-forming minerals (Doventon, 1994).

The Niger Delta is situated in southern Nigeria between latitudes 3° N and 6° N and longitude 5° E and 8° E (Nwachukwu, and Chukwura, 1986), however, the study area, I-field, is located between latitudes 4.7950°N and 4.8186°N, longitudes 6.9595°E and 6.9800°E. The onshore portion of the Niger Delta province is delineated by the geology of Southern Nigeria and Southwestern Cameroon. The northern boundary is the Benin flank; an east-northeast trending hinge line south of the West Africa basement massif. The northeastern boundary is defined by outcrops of the Cretaceous on the Abakaliki High and further east-south-east by the Calabar flank; a hinge line bordering the adjacent Precambrian. The province covers 300,000 km<sup>2</sup> and includes the geologic extent of the Tertiary Niger Delta (Akata-Agbada) petroleum system (Tuttle *et al*, 1999). Figure 1 shows the geological map of Niger Delta.

The Niger Delta is situated in the Gulf of Guinea and extends throughout the Niger

Delta province (Klett *et al.*, 1997). From the Eocene to the present, the delta has prograded south-west ward, forming depobelts that represent the most active portion of the delta at each stage of its development (Doust and Omatsola, 1990). These depobelts form one of the largest

regressive deltas in the world with an area of some 300,000km<sup>2</sup> (Kulke, 1995), a sediment volume of 500,000km<sup>2</sup> (Hospers, 1965) and a sediment thickness of over 10 km in the basin depocenter (Kaplan *et al.*, 1994).

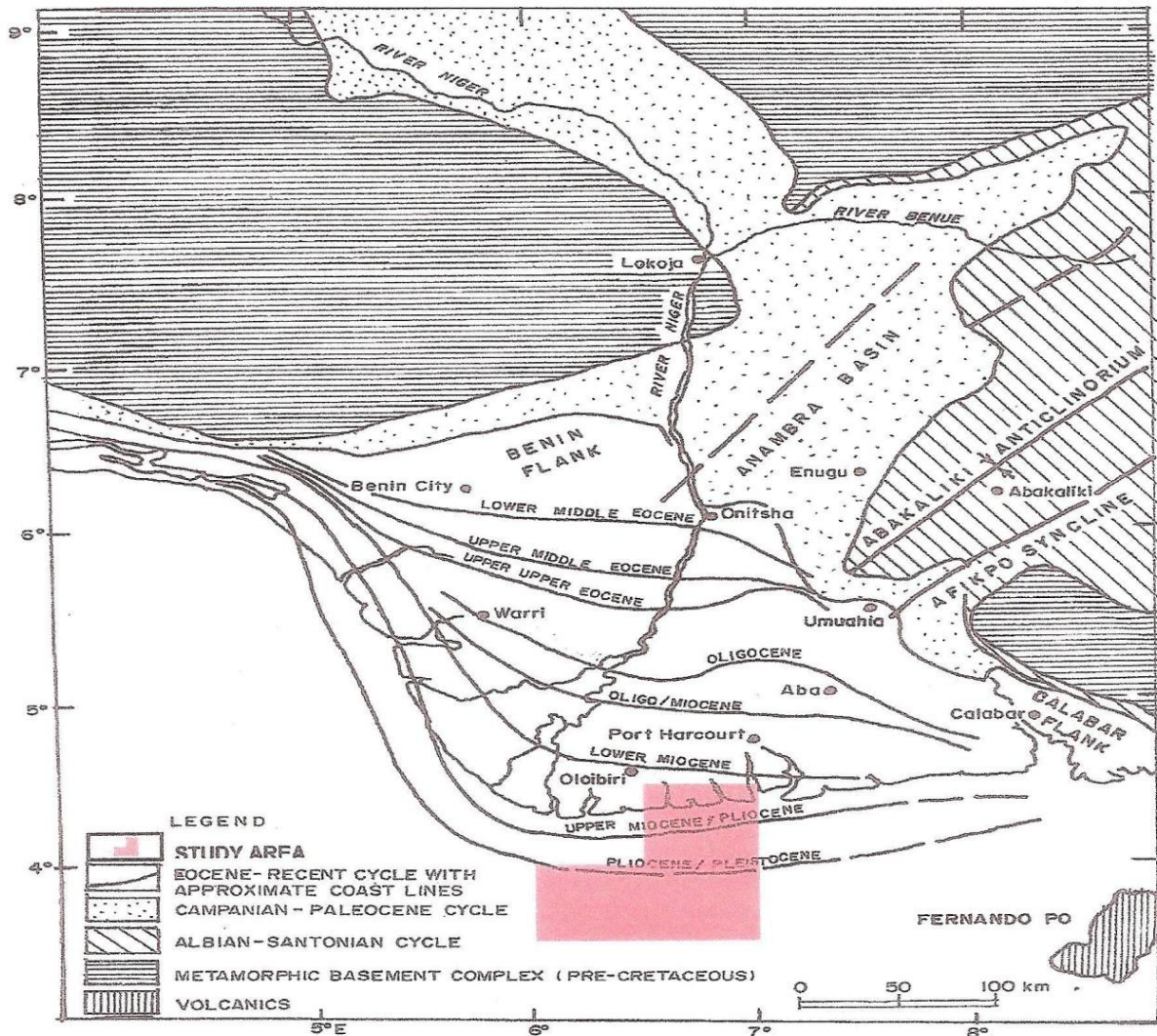
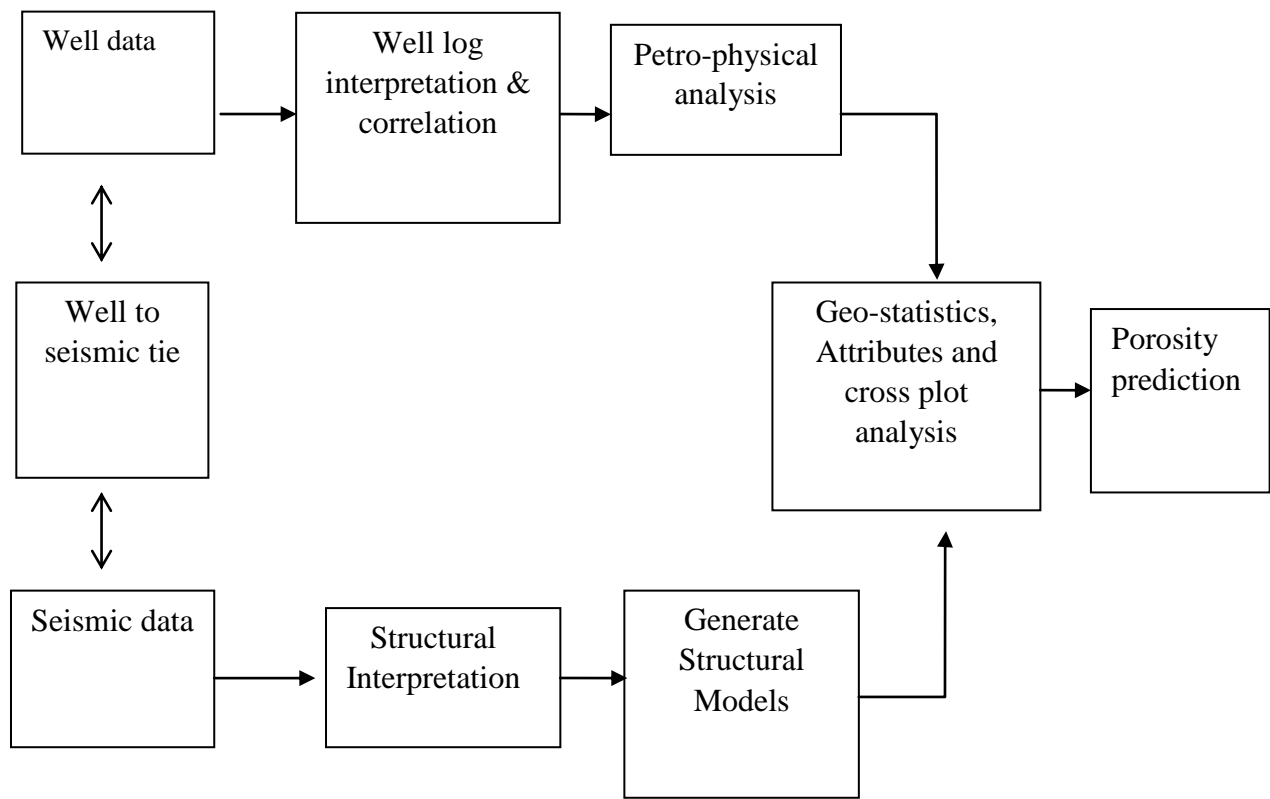


Figure 1: Generalized geological map of Niger Delta basin (Okiwelu and Ude, 2012)

**Workflow**

For the purpose of this study, a particular workflow method was followed to arrive at

the final point of being able to predict the porosity of I-field. The structure of the workflow is shown in figure 2.



**Figure 2:** Workflow for data analysis

The first step will be identifying the reservoir amidst the data available, hence the need to begin with the well data as it gives the log motif of I-field which includes the gamma ray log, resistivity log, density-neutron log, acoustic impedance log, among others. Seismic data is also imported which contains the raw data derived from the seismogram attained during acquisition on the field. Figure 3 shows well-log data that have been imported which comprises of various petro-physical parameters such as Gamma-ray log and Resistivity log which

help measure the gamma and resistivity values respectively. Figure 4 and figure 5 are both seismic data that have been imported, figure 4 gives the section of the seismic trace that have been observed from the top of the surface while figure 5 shows the section of the seismic trace that has been observed from a deeper area within the sub-surface. It is observed in figure 5 that this section is characterized by various faults and amplitudes of different variations below the sub-surface.

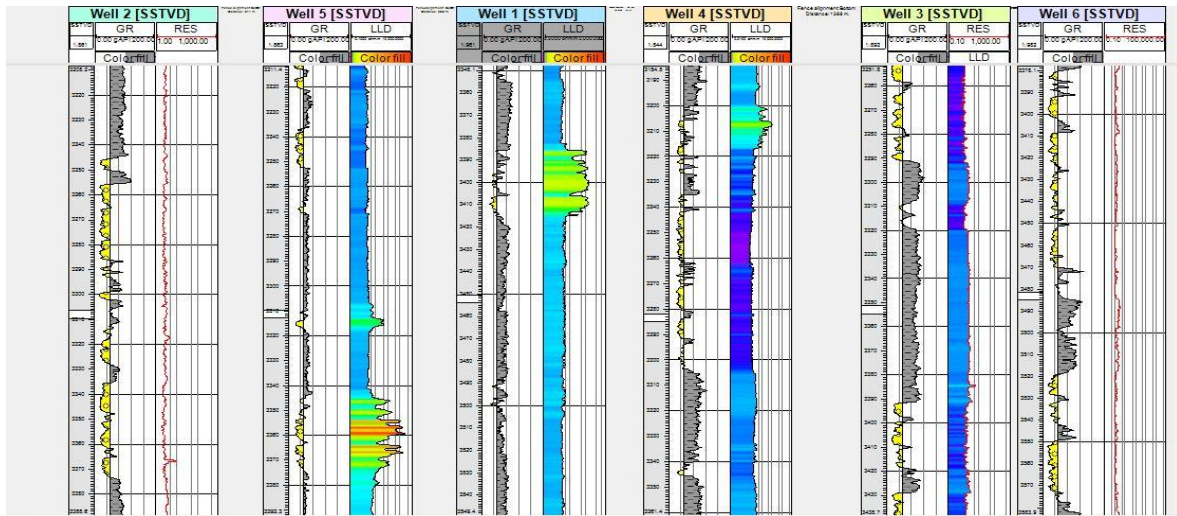


Figure 3: Well data after import (GR represent gamma-ray log, RES and LLD represents resistivity log)

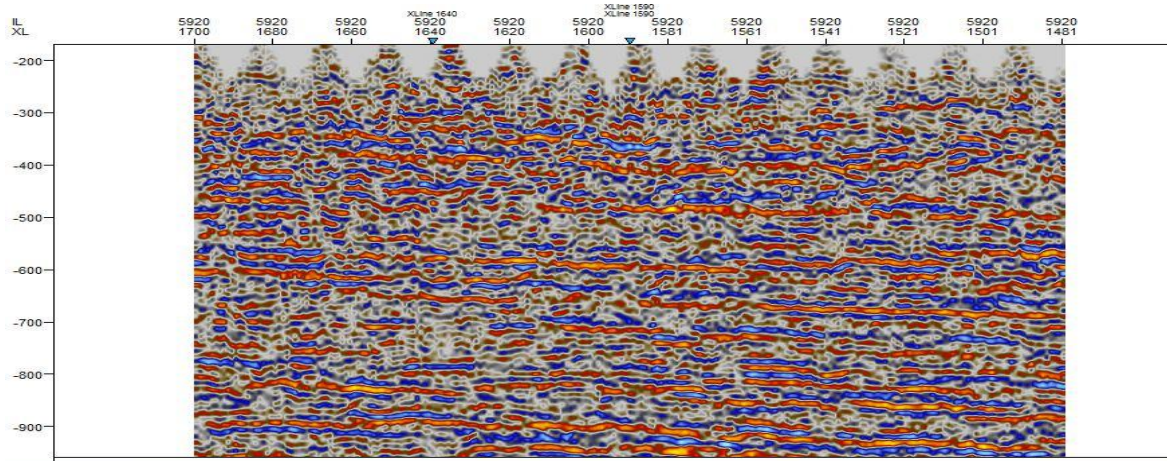


Figure 4: A section of seismic trace from the surface

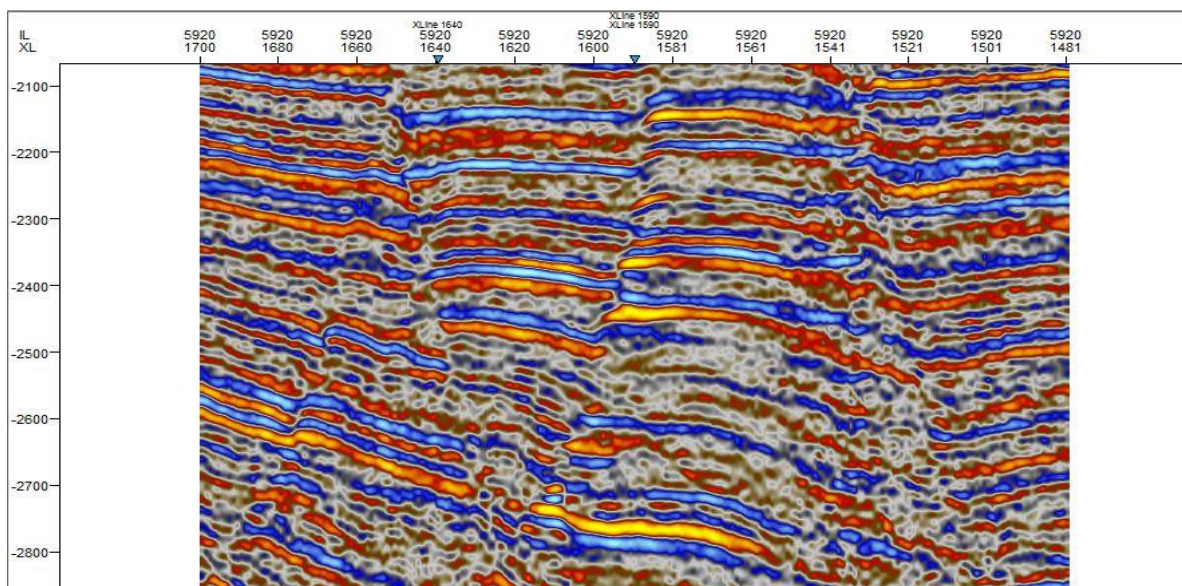


Figure 5: A deeper section of the seismic trace characterized by faults and high amplitude

## RESULTS

### Well Log Data Import and Interpretation

In processing and interpreting data for the exploration wells, well log data for each of the wells was loaded into the well section window of the interpretation software. Figure 6 shows a typical loaded well log data for a particular well; this time, well 4. The different calibrations that have been extracted for that particular well is observed, for example, the gamma ray log that describes the lithology of the area by showing the gamma content; given that low

gamma signifies a sandstone formation while high gamma signifies a shale formation.

Next, the density-neutron log is also observed; this helps to identify the type of fluid content present in the formation which could be filled with either gas, oil or water. The density log determines the amount of electron density within the formation by quantifying the number of emitted gamma rays that collide with the electrons in the formation and got scattered.

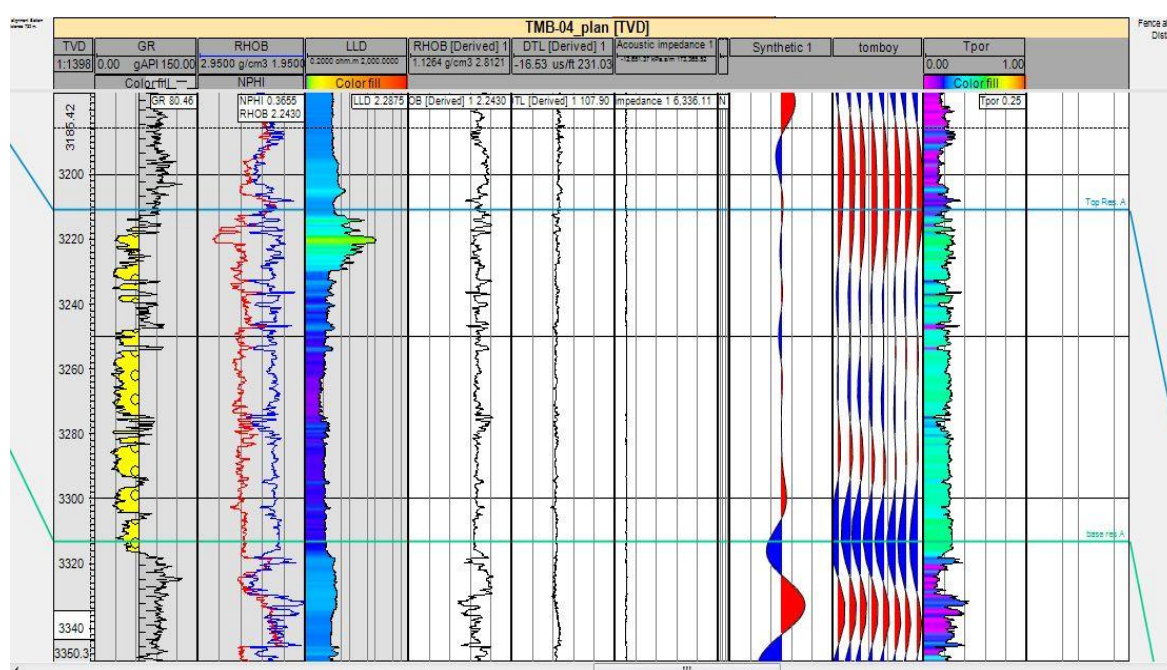


**Figure 6:** Well log data for well 4 after being loaded on the well section window of the Petrel software

The neutron log, which is also taken, helps to identify the amount of hydrogen concentration within the formation. In figure 6, the density-neutron log is a crossover, this is because water has a higher density than oil and gas; it also has a higher neutron value than oil and gas. Hence, the formation of hydrocarbon content is identified through formations that have a balloon shape density-neutron log which indicates that

such formation has low density and low neutron value.

The resistivity log is also observed amongst the loaded well data. This helps to separate formations that contain water from formations that contain hydrocarbon. A peak in the resistivity log in figure 6 is noted as hydrocarbons have a higher value of resistivity compared to water whose resistivity value is low.

There are other logs whose measurements have been taken into account, but however, may not be necessary for the purpose of this research. Some of these logs include depth log, caliper log, water saturation log, sonic log, among others.

All these logs can be used to identify formations with amplitude variation below the subsurface of the earth. They can also be used to generate acoustic impedance and in turn a synthetic seismogram which is the true representation of the seismic traces attained below the subsurface as opposed to the data obtained from the seismograph during the acquisition of seismic data. The synthetic seismogram and the data obtained from seismic acquisition will be compared in the well to seismic tie phase.

It is important to note that two lines are visibly cutting across the well section; these are lines that map the top and base of the reservoir formation as obtained from all the logs from which data have been extracted. This is one of the most important reasons for uploading the well log data so as to help

in separating formations that contain hydrocarbon from those containing water, and also to identify reservoirs in I-field that exist within the vertical formation of the sub surface.

### Well Log Correlation

It is important to determine how laterally distributed our identified reservoir formation is within the sub surface. In figure 7, the result for well correlation is achieved. Multiple reservoirs within the subsurface have been identified, and a particular reservoir tagged Reservoir A has been marked bounded by the top and base lines as shown in figure 7. However, because of the scope of this research work which is to predict porosity across the whole of I-field, it is necessary to determine a lateral extent of the reservoir formation as opposed to only the vertical extent of the sandstone formation within the reservoir that have been identified in the well section. The gamma ray and resistivity logs were used to delineate the wells since both logs present qualities that satisfy the aim of this process.

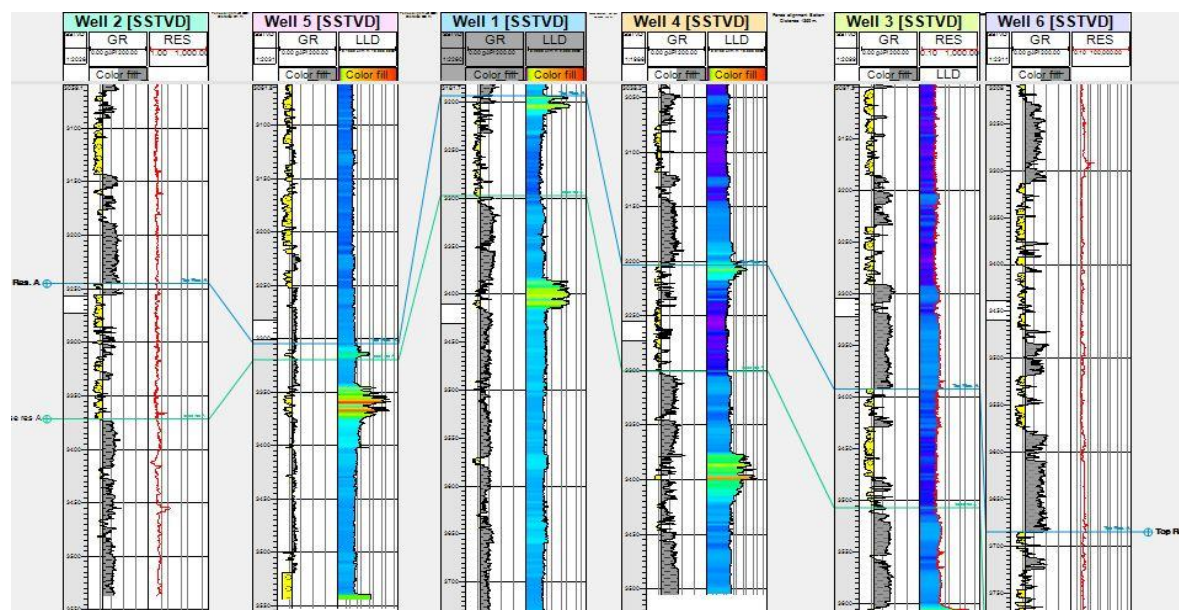


Figure 7: Well log correlation of the six wells within I-field

The gamma ray log was used to identify the shale/clay formation and also the sandstone formation across all the six wells that penetrate I-field at different locations while the resistivity log was used to identify the presence of hydrocarbon content within the said formation.

Chrono - stratigraphy correlation that involves using the log motif of the shale/clay formation is used to ensure that the same reservoir is observed across the six wells because unlike sandstone formations, shale formation is laterally extensive and is less prone to changes as a result of its non-porous nature. It is possible to observe the same shale across all wells than to identify the same sandstone formation across the six wells.

There is an upward and downward trend in reservoir variation across the six wells and not necessarily side by side in terms of depth, this can be as a result of the different faults acting below the subsurface within I-field. Some sandstone formations are of little volume visually (well 5) compared to what was obtained in some other wells (well 2 & well 4) while the shale/clay formation look almost similar across the six wells. This shale acts as a seal for the reservoir. The shale above the reservoir or the shale below the reservoir can therefore be used to correlate the well log data.

### **Well to Seismic tie Interpretation**

Well to seismic tie was carried out using a synthetic seismogram that is generated from

the convolution between acoustic impedance and extracted wavelet. The acoustic impedance log is formed by combining check-shots data with corrected density and sonic logs.

When the synthetic seismogram is attained, it is placed side by side with the composite seismic traces derived from acquisition, both data can then be compared. The tie between both the peak and trough of the seismic traces is observed from both data. From figure 8, by comparing the synthetic seismogram and the composite seismogram, the level of seismic tie is not quite appreciable as there is less than about 50% tie of the traces. Another notable feature in this tie is an overlap of both the peak and trough traces, this feature is known as “Tuning effect” or “Aliasing” (an effect that causes multiple signals to be like each other, that is, they become indistinguishable).

The tuning thickness is the bed thickness at which two events become indistinguishable in time, it can be expressed mathematically as:

$$Z = \frac{V_I}{2.8f_{\max}} \quad (2)$$

where  $Z$  = tuning thickness of a bed, equal to  $\frac{1}{4}$  of the wavelength

$V_I$  = interval velocity of the target  
 $f_{\max}$  = maximum frequency in the seismic section (Schlumberger oilfield glossary, 2013)

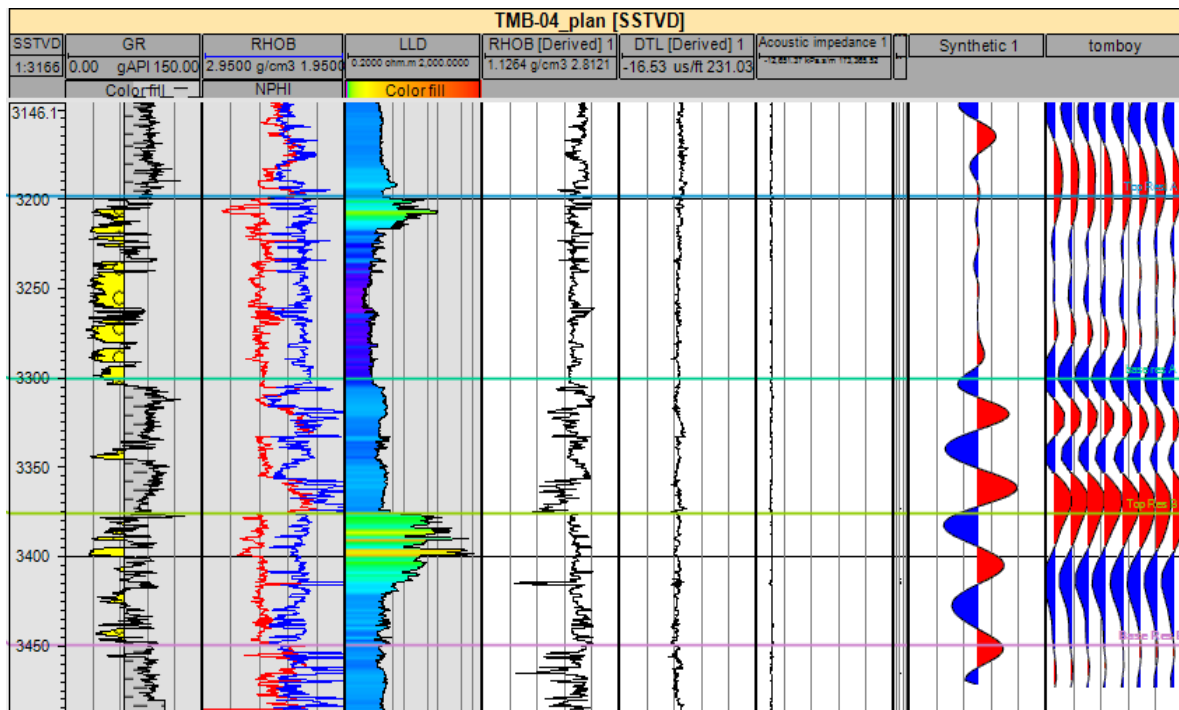


**Figure 8:** Well to Seismic tie in well 4 formation

### Structural Interpretation

Once the reservoir to be delineated is identified from the well logs, petrophysical analysis to determine the porosity values within the six wells could be carried out. Figure 9 shows how each inline and cross line visually behaves when horizons and faults associated with that particular grid have been picked; the same goes for the whole seismic grid comprising of about 65 sections for both inline and cross line. Figure 10 shows the result obtained from manually picking the horizon at the top of the reservoir.

Some interesting anomalies in the interpretation window in figure 9 is observed, such as the amplitude of seismic traces and the various types of faults that delineate the formation below the subsurface. The categories of faults found in this formation are both the normal faults and

the reverse faults. A fault is described as the discontinuity in the volume of a rock, along the fractures across which there has been significant displacement as a result of the movement of the earth.

For a normal fault and reverse fault as characterised in our formation above, the hanging wall is noted moving downwards relative to the footwall for the normal fault while in the reverse fault, the hanging wall is moving upward relative to the footwall. This is what is visible in figure 9 above as faults 2 and 4 describes the normal faults while faults 1 and 3 describes the reverse fault. The direction of the faults was also identified.

Figure 11 shows the end result of manually picking the horizon and faults across the survey area and developing a structural framework of how the reservoir is expected to be viewed from the top of the reservoir.

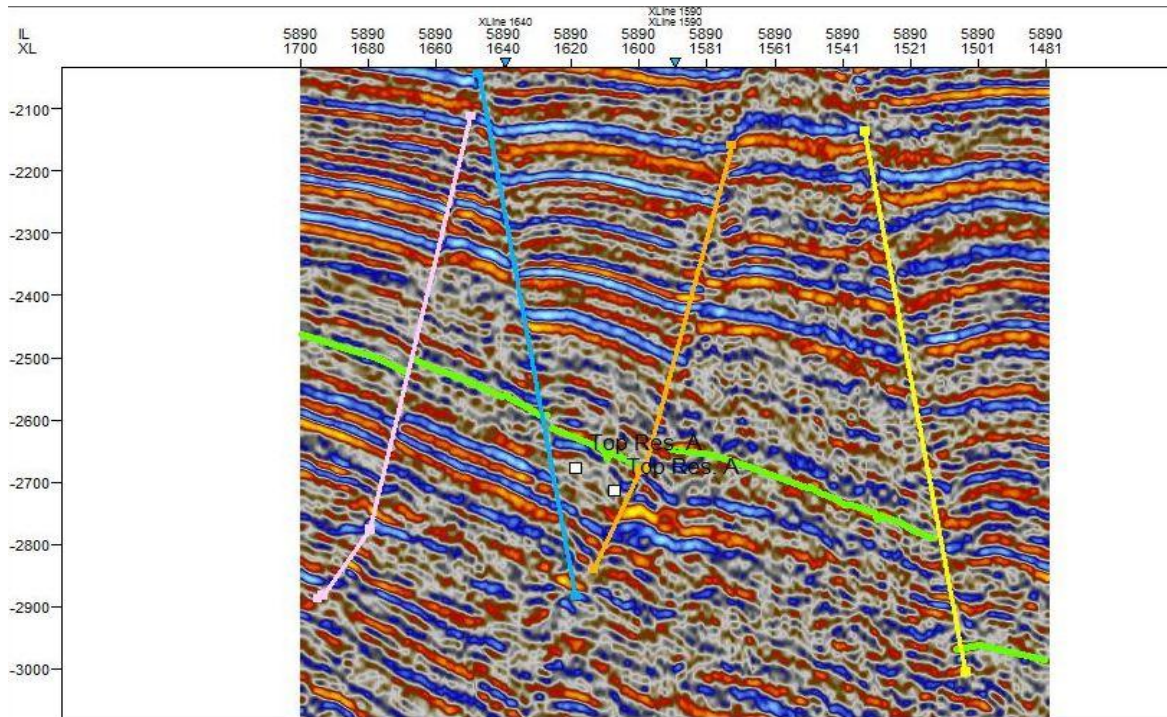


**Figure 9:** Interpretation window showing the horizon delineating the top of the reservoir and the different faults acting below the subsurface characterising the geology of the area

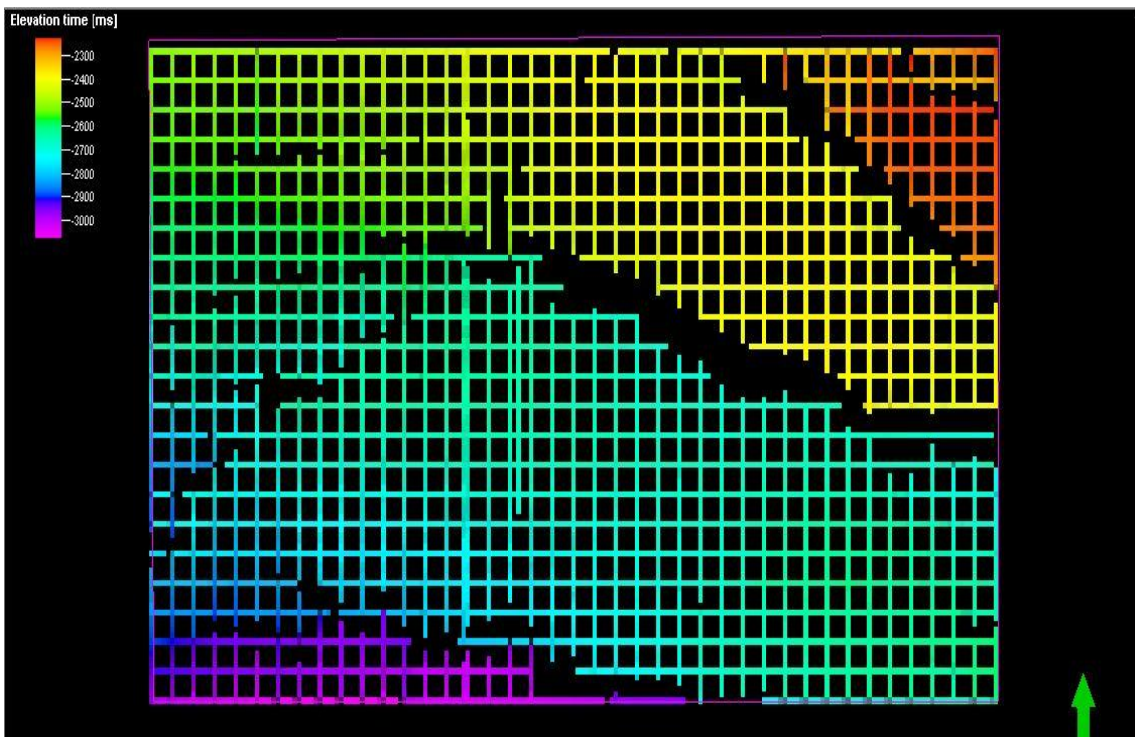


**Figure 10:** Seismic grid of the study area showing horizon pick across the inline and cross line following a 10 \* 10 grid positioning

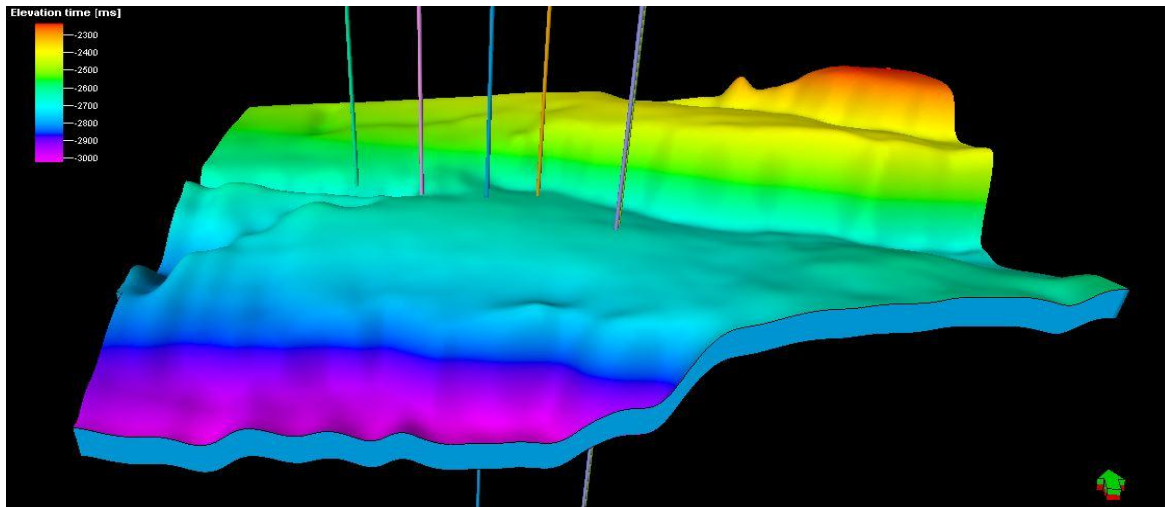


**Figure 11:** 3-D view of the reservoir model (structural framework) in time showing the boundaries of the reservoir along the survey area.

**Time and Depth Map Interpretation**

Figures 12 and 13 show the time map and depth map respectively, of the top of the reservoir. Gradually the reservoir begins to take shape and the true structural form of the survey area is observed below the subsurface, within the time/depth map where contours have been formed. It is observed that close contours could represent traps for hydrocarbon content as delineated by the petroleum system of the Niger Delta region.

Most of the traps of the Niger Delta are fault supported hence more interest will lie on areas where there is a contour closing on a fault and characterized by a peak in resistivity on the resistivity log. Further tests such as fault synch analysis, among others, can be carried out to confirm if it is a trap for hydrocarbon deposits. For the purpose of this research work, in identifying areas of high porosity, locations with closed contours are noted as they are likely to be areas of high porosity values.

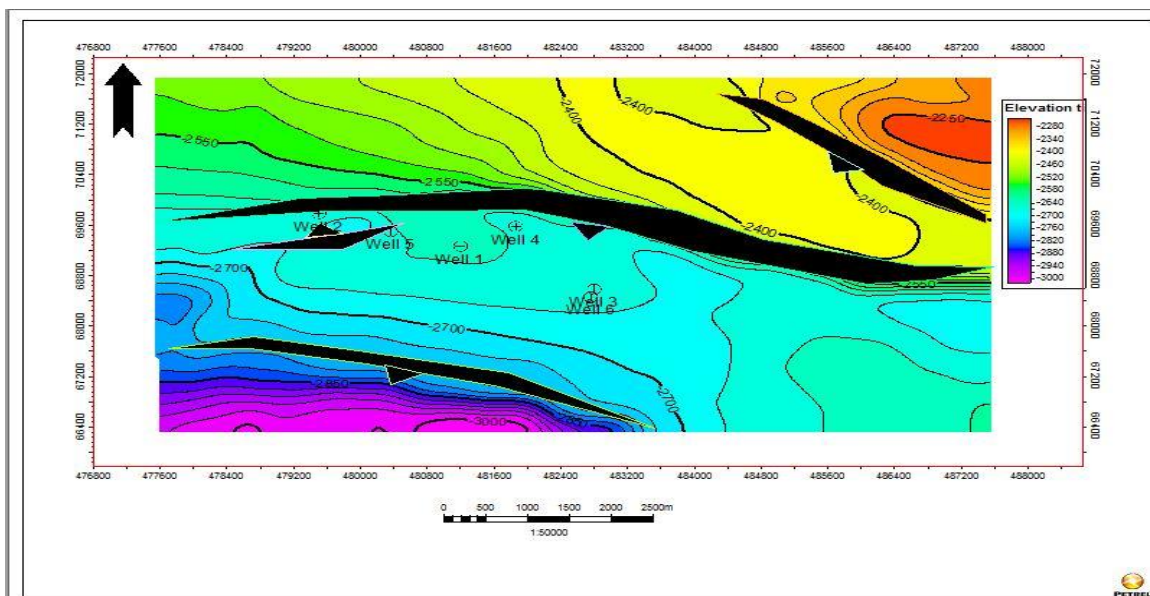


**Figure 12:** Time map of the reservoir top

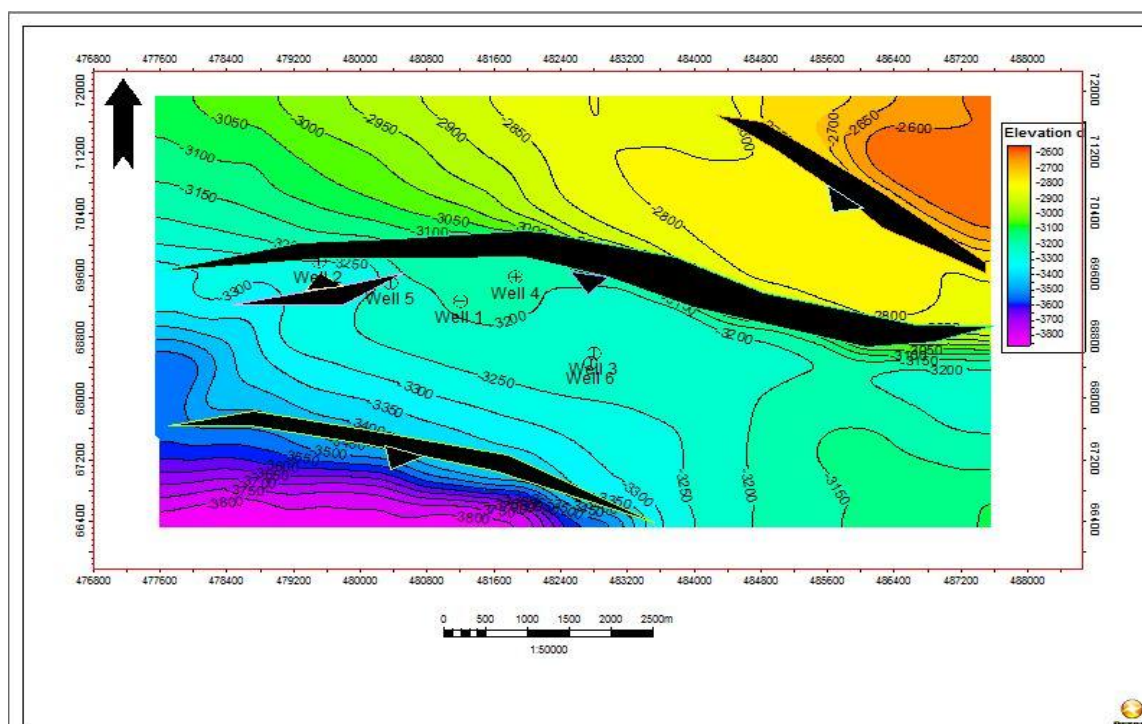


**Figure 13:** Depth map of the reservoir top

The direction of the fault planes was also observed in the time and depth map of figure 12 and 13. The fault planes are characterized by the black bold lines cutting across segments of the study area, four distinct faults were identified (F1 delineating an elevation area of -2800 to -3150, F2 delineating -3200 to -3400, F3 delineating a segment within the contour values ranging between -3250 and -3300, F4 delineating -3400 to -3800). The upward and downward throws of the fault are also included in the maps, with faults F1, F2 and F4 having a downward direction and a dip, however, F3 has an upward throw closing on fault F1.

To generate the depth map as in figure 13, a velocity model is developed. It makes use of check shots data (a type of borehole seismic data designed to measure the seismic travel time from the surface to a known depth;

Schlumberger, 2014) and converts each individual value of time into depth. This is necessary because the drillers are interested in depth when ready to drill in the formation during production of hydrocarbon. However, since seismic data is recorded in time, there is a need to convert the values extracted in time into depth. Basically, what is done is that, a time value that corresponds with the nearest check shot value is identified and a simultaneous equation to determine the corresponding values for the depth of that time value is achieved.

For example, to determine the depth value of 2460s knowing the nearest check shot value in time and depth to be 2478ms ~ 9518m, from our calculations, there is an equivalent of 9449m ~ 2460ms. At the end of which gives a corresponding value in depth for the horizon (top of well) for each of the wells as shown in figure 14.

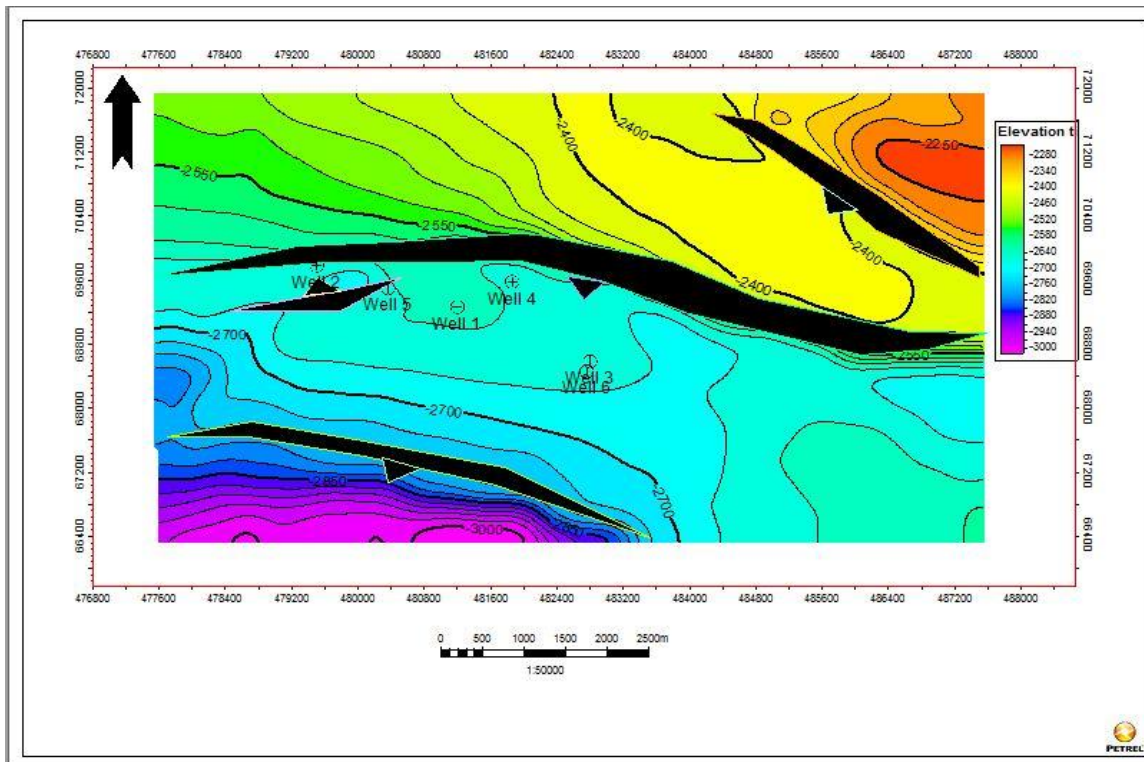


Figure 12: Time map of the reservoir top

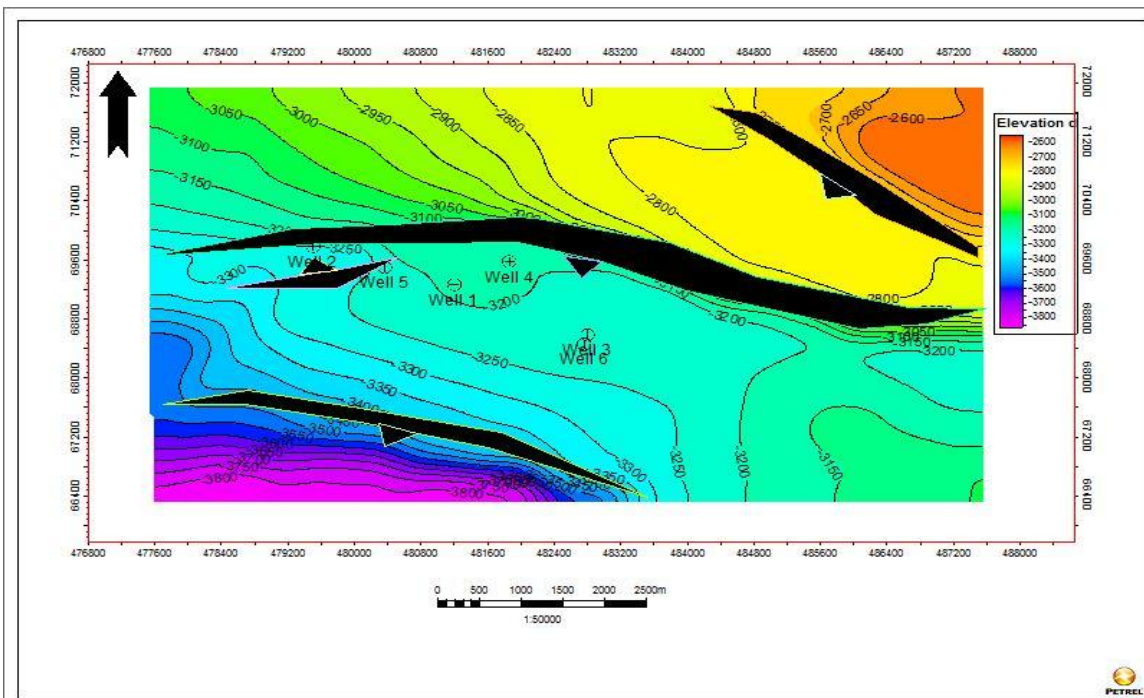


Figure 13: Depth map of the reservoir top

	A	B	C	D	E	F	G	H	I
1	Velocity model	Velocity model							
2	User name	user							
3	Project	part 2.pet							
4	Date	Friday, June 20 2014 13:15:19							
5	From:	TWT [ms]							
6	To:	Z [m]							
7	XY:	[m]							
8									
9	TWT	Well	X-value	Y-value	Z-value	Horizon after	Diff after	Corrected?	Information
10		TMB-02_plan	479500.0	69800.0	-3244.71	-3244.71	0.00	No	
11		TMB-05_plan	480365.0	69515.0	-3308.75	-3232.73	-76.02	No	
12		TMB-6I_plan	482759.0	68478.0	-3684.54	-3216.35	-468.19	No	
13		TMB-01_plan	481200.0	69280.0	-3192.96	-3192.96	-0.00	No	
14		TMB-03/st_plan	482800.0	68600.0	-3391.63	-3214.91	-176.72	No	
15		TMB-04_plan	481860.0	69595.0	-3198.02	-3198.02	0.00	No	

**Figure 14:** Velocity model showing conversion from time to depth of horizon (column E is depth of reservoir top from Well Logs while column F is depth of reservoir top from Seismic Sections)

### Porosity Model Analysis

Once the structural framework was generated by giving a volume to the reservoir with edges surrounding the top and base of the reservoir and faults interplaying within the formation, the next step was to generate the porosity model using this structural framework and geo-statistics. The structural framework is composed of small cells called geo-cells which could be thousands or millions within the reservoir model and these geo-cells are attributed with values. In the methodology, the wells were up scaled where each cell within this framework that is penetrated by a well is attributed with a discrete porosity value extracted; hence for all wells, there is a discrete porosity value for each geo-cell that is penetrated. However, there are still no values for areas where there are no wells

and here geo-statistical analysis is done. The geo-statistics method that are applicable here are Variogram analysis and Sequential Gaussian simulation. When geo-statistics is done, a model is achieved as shown in figure 15. There are multiple realizations as shown in figure 16 since Sequential Gaussian Simulation is probabilistic and the best realization that describes the porosity model desired is selected.

Figure 17 shows the faults included in the porosity model, the faults supports the traps formation as the contours close around the faults as earlier seen in figures 11 and 12. The porosity model reveals an area of high porosity at the -2800 m contour as to the -3200 m contour closing on the fault F2 plane.

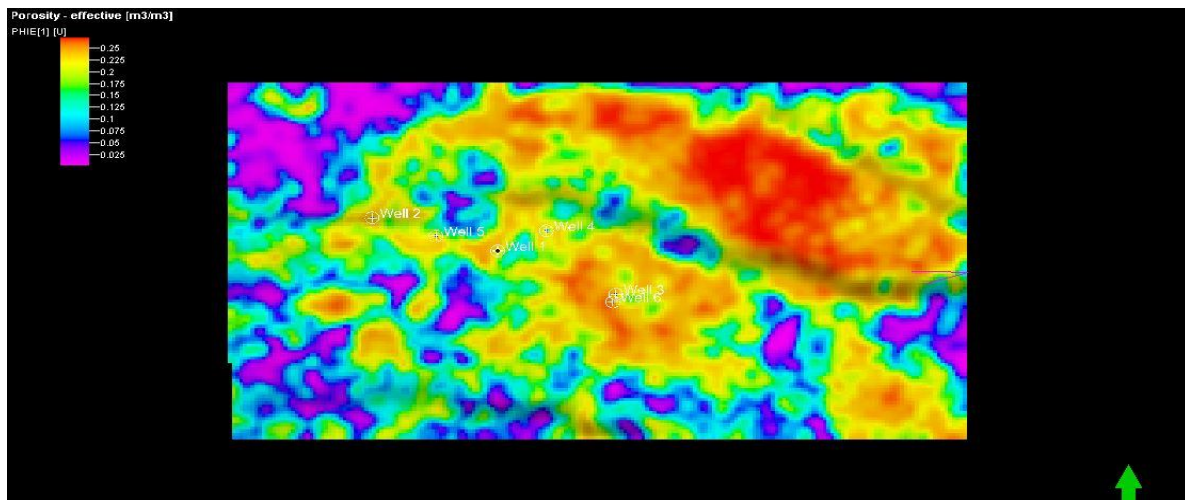


**Figure 15:** 2-D Porosity model for survey area showing wells penetrating the reservoir

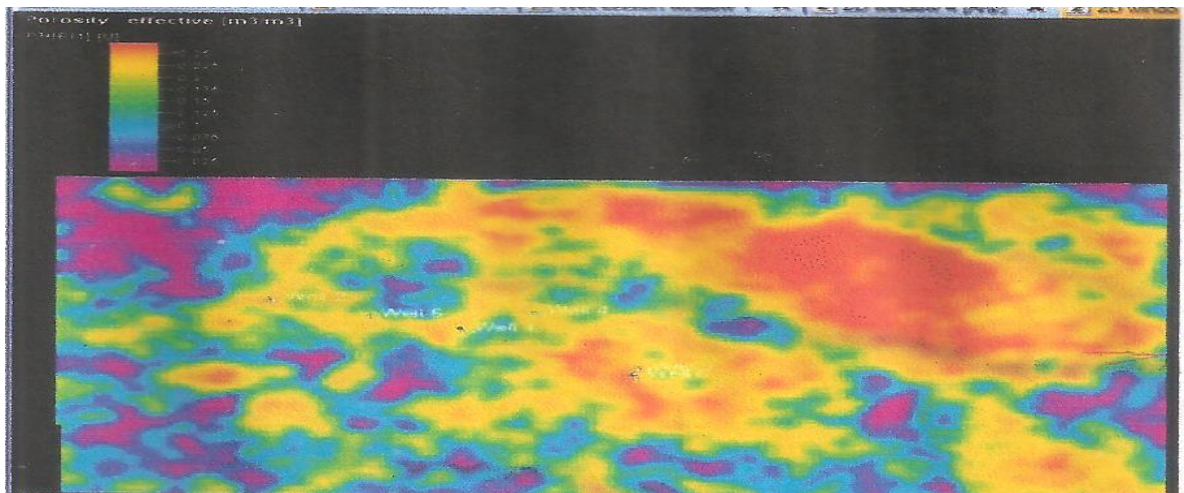


**Figure 16:** Petrel model window showing multiple realizations of porosity model analysis generated by the Sequential Gaussian Simulation

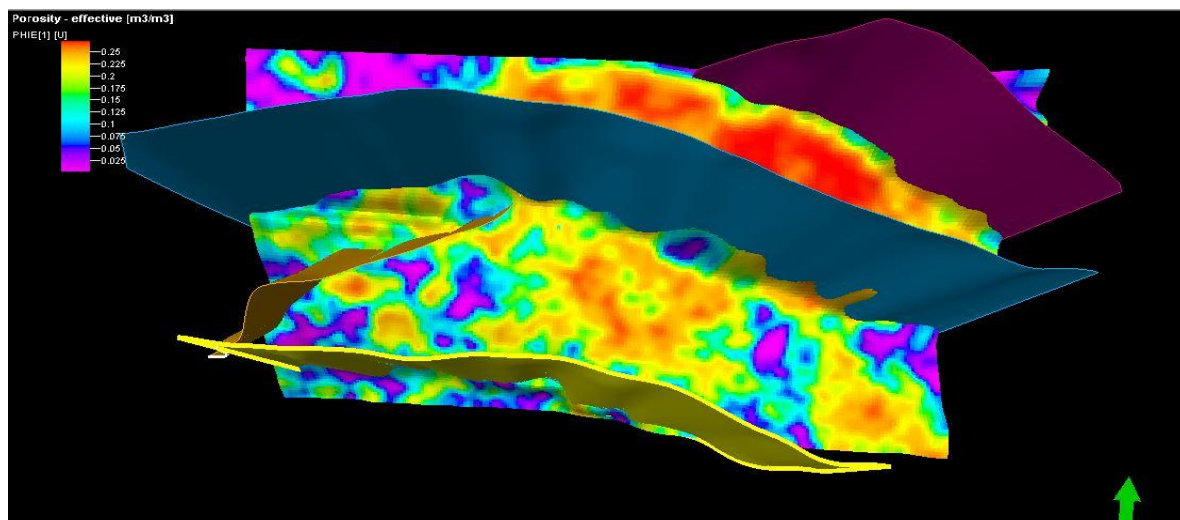


**Figure 17:** 3-D porosity model showing fault planes that interplay within the formation

### Envelope Attribute Analysis

Areas of high amplitude can be suggested to be areas of increased porosity due to the increased reflection strength observed in such areas. It is observed in figure 15 that there exist some bright spots that depict high amplitude variation with other formations within the subsurface, however for a clearer view as to the representation of what is seen, the result is constrained with the envelope attribute because of its relationship with amplitude. It is also seen in figure 18 that areas of suspected increased porosity values reveal bright spots mostly at depth 2800 m which forms an area of interest as a result of the anomaly in this

region and also at depth 3200 m located in the central region of the survey area where some of the exploration wells have been sited close to the fault plane interplaying within the formation.

If the regions where the wells are located in this model are compared with the porosity values derived from the well logs, there will be a significant similarity as it is known that porosity always mimic the kind of depositional environment within the formation. Hence, a shale strata will mimic regions of low porosity while regions of sandstones deposition will display regions of high porosity.

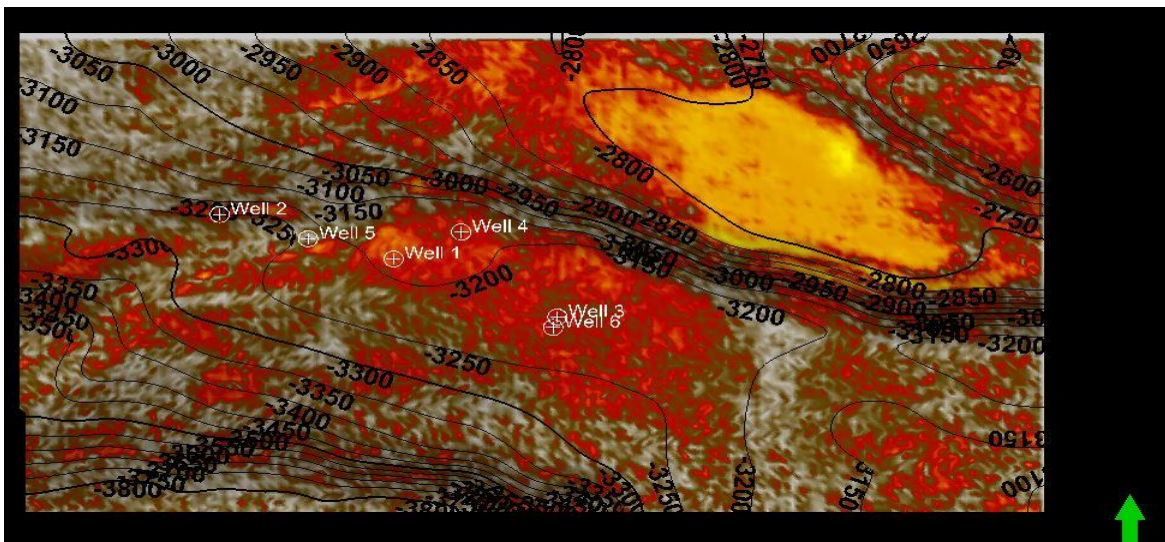


Figure 18: 2-D porosity model incorporated with Envelope attribute

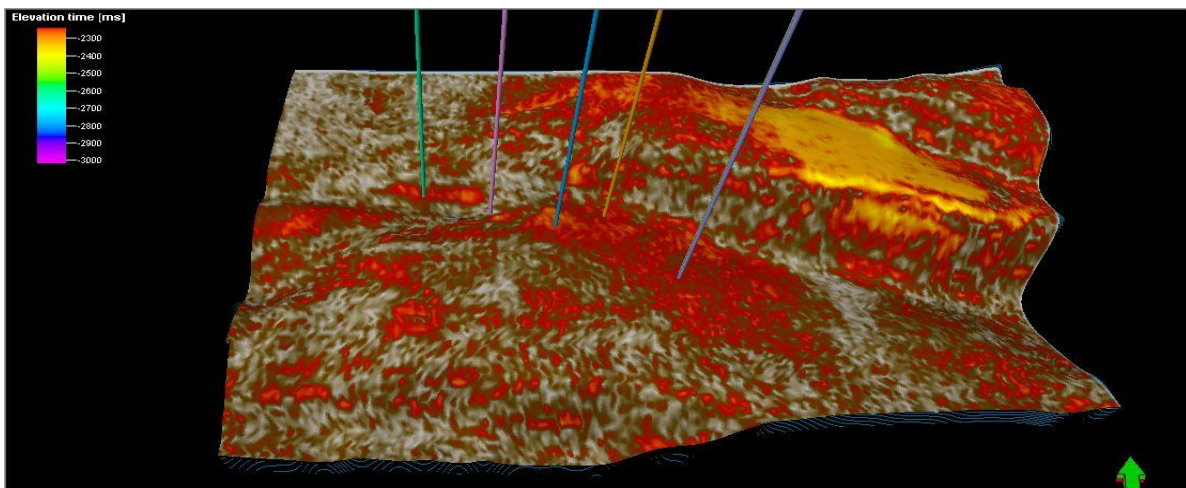


Figure 19: 3-D porosity model incorporated with envelope amplitude attribute

### Root Mean Square Amplitude Analysis

Root Mean Square amplitude attribute is an attribute that is computed over a time window independently for each trace which unlike some other attributes based on time associated with multiple horizons, derives its results from a single horizon. Mostly, its time window is always over 24 ms (Pennington, 1997). Figures 20 and 21 respectively show the 2-D and 3-D Root Mean Square (RMS) amplitude attribute guided porosity model. The horizon being taken into consideration here is the top of

the reservoir and the results is seen in figure 20 as the variation in the amplitude becomes clearer and the upward progression (North-East) of porosity becomes more visible.

Areas of suspected increased porosity values reveal bright spots mostly at depth 2800 m just as in figure 19, which forms an area of interest as a result of the anomaly in this region and also at depth 3200 m which is located in the central region of the survey area where some exploration wells have penetrated the formation.

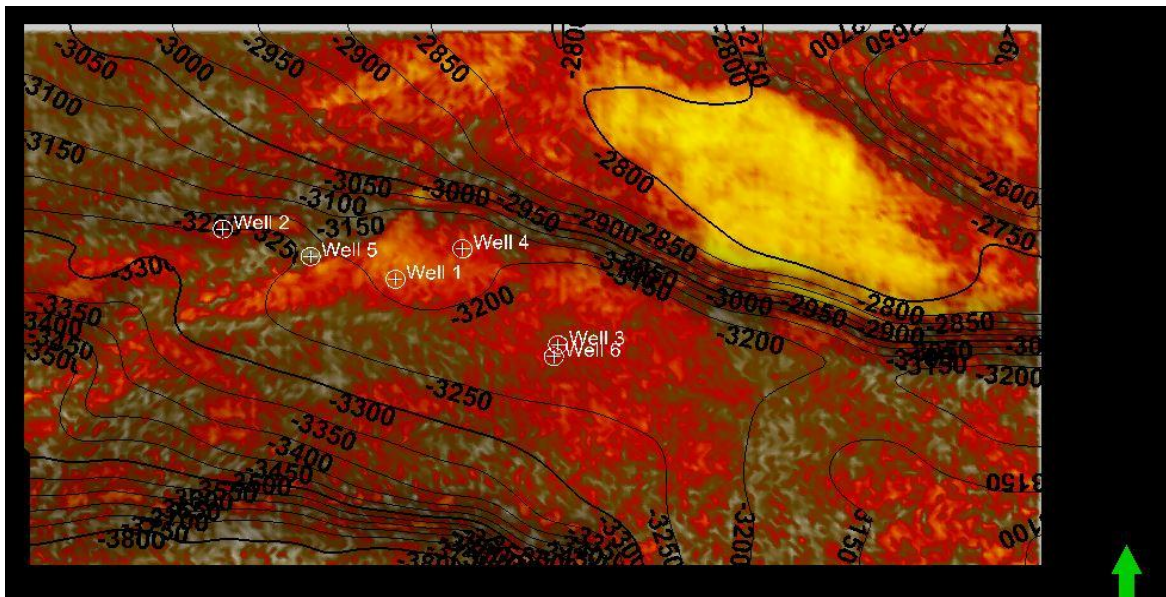


**Figure 20:** 2-D porosity model incorporated with RMS amplitude attribute

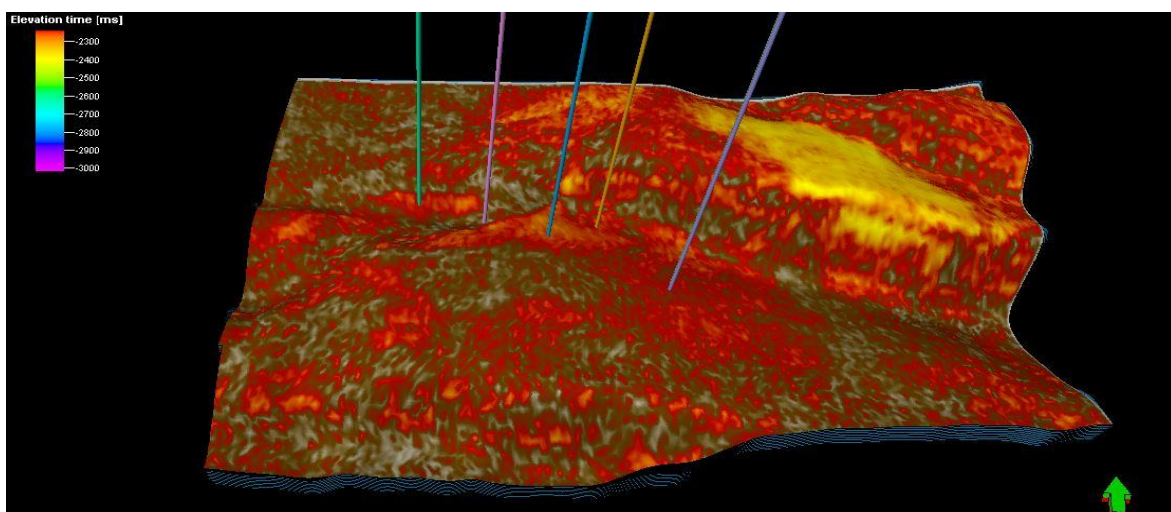


**Figure 21:** 3-D porosity model incorporated with RMS amplitude attribute

### Cross-Plot Analysis

Figure 22 shows the crossplot of the porosity log with gamma ray log that describes the relationship between these two parameters. At the distinguishing value of the gamma ray log that separates the sandstone formation from the shale formation, there is a distinction in the

variation of porosity from both formations as was observed in the increase in porosity for the lower gamma ray values of 0 to 55 and a decrease in porosity from the upper gamma ray values of 55 to 150. This goes to prove that in the sandstone formation, the porosity is high as compared to the shale formation that has low porosity.

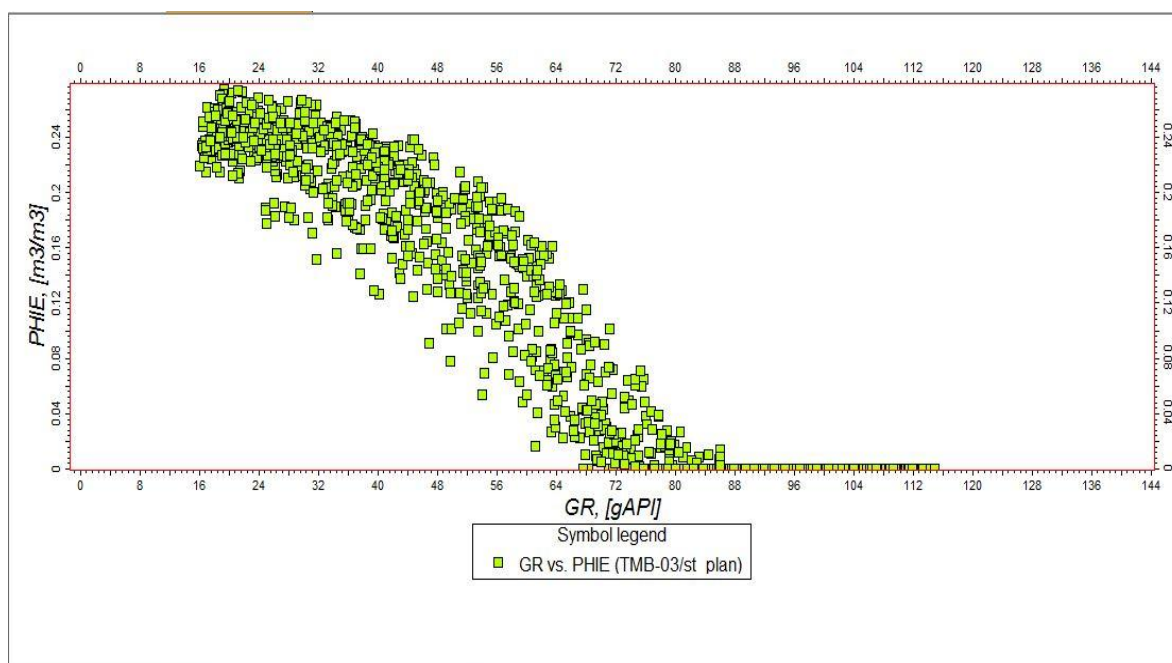


**Figure 22:** Crossplot of Porosity with gamma ray log

### DISCUSSION

This study has developed a framework by which the porosity of formation within an exploration field, in this case the I-field could be determined using seismic attributes and geo-statistics methods. From this study, a lot has been achieved with this process of incorporating well-log data and seismic attributes in predicting porosity. When the well-log data was loaded into the PETREL software used, multiple reservoirs were identified beneath the subsurface of I-field as a result of the peak variation in resistivity increase. Gamma ray log helped in identifying lithology distinguishing between sandstone formation and shale formation. The density-neutron log was used in

identifying the fluid content as hydrocarbon. This study has been used to delineate the reservoir identified, as the well logs of the formation were correlated using the log motif of the shale to be able to observe how laterally extensive is the identified reservoir within the formation.

Time and depth maps of the reservoir were generated and how the fault planes affect the formation down the depths were observed. Four different fault planes were observed, with three of these faults (F1, F2, and F4) having a downthrown while one (F3) has an up-throw direction. Closing contours at depth 2800 m and 3200 m were also observed.

Petro-physical analysis was carried out and the porosity values at each of these wells were extracted and then interpolated using Geo-statistical techniques (Variogram analysis and Sequential Gaussian Simulation) to determine values of porosity in areas where wells have not been drilled. When the fault planes were inserted in the porosity model generated, the porosity distinction was observed from the depth of 2800 m with porosity value of 28% to 3200 m with porosity value of 18%, probably as a result of the fault plane located within the formation as compaction could have resulted from residues moving towards the lower depth.

Envelope attributes and Root Mean Square attributes were the seismic attributes selected to be used because of their direct relationship with amplitude of the seismic data. The formations where closing contours were discovered also have high amplitudes from the attributes analysis. This is a little bit similar to the porosity models derived, but with enhanced parameters as in amplitude variation between the two models. This helps to predict, with a high level of certainty areas that are very porous (28%) within the field and hydrocarbon can be extraction from this areas at depth of 2800 m.

A crossplot between the porosity of the field and the gamma ray log which predicts lithology was done, an increasing trend in porosity values is exhibited at the boundary between the sandstone formation and shale formation with a value of 55%.

The information derived in this study is useful in a number of ways such as in the prevention of accidents in form of explosions when drillers hit a gas pocket.

This is achievable because the exact depth of hydrocarbon deposits would have been estimated and the fluid content at that depth would have been determined from further analysis. Closures observed within the models can be predicted as prospects or sweet spots for hydrocarbon holes that have not yet been drilled for hydrocarbon extraction in I-field. It was observed that the location of the drilled wells occurred at a depth of 3200 m where there is a contour closing in on the fault at the centre of I-field. However, other closures within the field such as at depth 2800 m closing in on another fault and at the depth 3150 m at the South-East direction are prospects for hydrocarbon extraction because of their high porous characteristics as predicted in the model.

With the many important characteristics of formations within the subsurface that can be used to determine locations of hydrocarbon reservoirs below the earth surface, this work has used porosity characteristics of formations to determine locations of hydrocarbon reservoirs of I – field in the Niger Delta Area.

## REFERENCES

- Alao P. A., Nwoke C.E., S. O. Olabode S.O. and Ata A., (2014). Lithology and porosity heterogeneity prediction using multiple seismic attributes on 3-d surveys: an example from Edim oil field, Niger delta, International Journal of Advanced Geosciences. Vol. 2 (1), p 1 – 7.
- Bisht B.S.,Singh. RBN, BahugunaM.M., Das P.K., Shukla M., Mondal S. and Samir W. (2013). Stochastic Approach to Delineate Facies - An Integrated Study Using Seismic

- Attributes and Facies Logs on a Clastic Oil & Gas Reservoir of Western onland Basin of India: 10th Biennial International Conference & Exposition p146.
- Deutsch, C.V. (2002). *Geo-statistical Reservoir Modeling*, Oxford University Press, New York, p. 376.
- Doust H. and Omatsola E. (1989). Niger Delta. *American Association of Petroleum Geologists Memoir*, Vol. 48, p 201-238
- Doust H. and Omatsola E. (1990). Niger Delta AAPG Memoir 48, *American Association of Petroleum Geologists*, Tulsa. Vol. 48, p 239-248.
- Doveton J.H. (1994). Geologic log analysis using computer methods. *Am. Assoc. Petrol. Geol. Computer Applications in Geology* No 2, p 256.
- Dubruble O. (1998). *Geo-statistics in Petroleum Geology*. AAPG Education Course Note, Series #38.
- Hospers, J. (1965). Gravity field and structures of the Niger delta, Nigeria, West Africa: *Geological Society of America Bulletin*, Vol. 76, p 407-422.
- Kaplan A., Lusser C. U. and Norton I.O., (1994). Tectonic map of the World, panel 10: Tulsa, *American Association of Petroleum Geologists*, scale 1:10.000.000.
- Kelkar, M. and Perez, G. (2002). *Applied Geo-statistics for Reservoir Characterization*, Society of Petroleum Engineers, Richardson, pg. 264.
- Klett T.R., Ahlbrandt T.S., Schmoker J.W., and Dolton J.L., (1997). Ranking of the world's oil and gas provinces by known petroleum volumes: U.S. Geological Survey Open-file report-97-463, CD-ROM.
- Kulke, H. (1995). *Regional petroleum geology of the world. Part II: Africa, America, Australia and Antarctica*: Berlin, GebrüderBorntraeger, 143-172.
- Leiphart, D.J., and Hart, B.S., (2001). Comparison Of Linear Regression And A Probabilistic Neural Network To Predict Porosity From 3-D Seismic Attributes In Lower Brushy Canyon Channeled Sandstones, southeast New Mexico, *Geophysics* 66, 1349-1358.
- Malvic T. and Prskalo S. (2008). Significance of the amplitude attribute in porosity prediction, Drava Depression Case Study. *NAFTA Vol. 59* (1), p39-46.
- Norkhamboot T. and Wongpornchai P. (2012). Porosity Prediction Using Seismic Attribute Analysis And Well Log Data In An Area Of Gulf Of Thailand, Department of Geological Sciences, Faculty of Science, Chiang Mai University, Chiang Mai, 50200, Thailand 38th Congress on Science and Technology of Thailand.
- Nwachukwu, J.I. and Chukwurah, P.I. (1986). Organic matter of Agbada Formation, Niger Delta, Nigeria: *American Association of Petroleum Geologists Bulletin*, Volume 70, pp 48-55.
- Ogiesoba, O. C., (2010). Porosity prediction from seismic attributes of Ordovician Trenton BlackRiver groups, Rochester

- field, Southern Ontario. The American Association of Petroleum Geologists. Vol. 94(11), p 1657-1672.
- Okiwelu A. A. and Ude I. A. (2016). 3D Modelling and Basement Tectonics of the Niger Delta Basin from Aeromagnetic Data  
[www.cdn.interchopen.com/pdfs-wm/37849.pdf](http://www.cdn.interchopen.com/pdfs-wm/37849.pdf)
- Pennington, W. D. (1997). Seismic Petrophysics—An Applied Science for Reservoir Geophysics. The Leading Edge 16 (3): p 241.
- Rouhani S., Srivastava R.M., Cromer M.V., Johnson A.I., Desbarats A.J. (1996). “Geostatistical Estimation: Kriging” Geostatistics For Environmental And Geotechnical Applications, American society for testing and materials.
- Schlumberger Oilfield Glossary 2014
- Schultz, P. S, Ronen, S. H. and Corbett, C., (1994) Seismic-Guided Estimation of Log Properties: Part 1: A Data-Driven Interpretation Methodology, the Leading Edge 13, 305-315.
- Tebo, J.M. and Hart, B.S. (2003), 3-D Seismic Attribute Study For Reservoir Characterization of Carbonate Buildups Using A Volume-Based Method, CSPG/CSEG Joint convention, June 2-6.
- Tuttle, M.L.W., Charpentier, R.R., and Brownfield, M.E. (1999), “The Niger Delta Basin Petroleum System: Niger Delta Province, Nigeria, Cameroon, and Equatorial Guinea, Africa”. Open-File Report 99-50-H. United States Geological Survey: Washington, D.C. 44.